Supporting Information

Prediction of high-T_c superconductivity in H_6SX under submegabar pressure

Xinyi Gu,[1] Kun Gao,[1] Jian Hao,[1] Jingming Shi,[1] Wenwen Cui,[1,*] and Yinwei Li[1‡]

[1] *Laboratory of Quantum Functional Materials Design and Application, School of Physics and Electronic Engineering, Jiangsu Normal University, Xuzhou 221116, China*

[*] Email: wenwencui@jsnu.edu.cn
[‡] Email: yinwei_li@jsnu.edu.cn

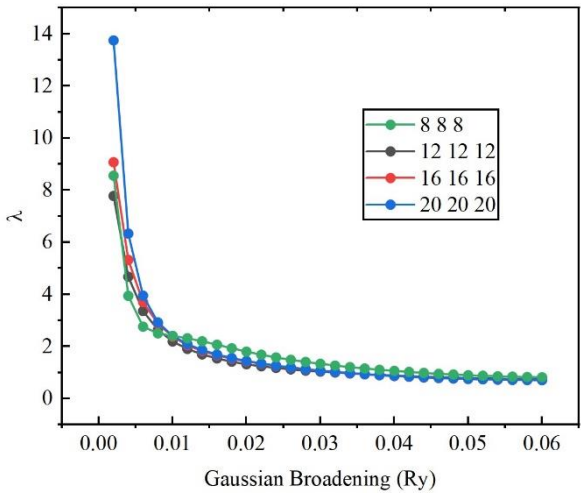

FIG. S1 Energy Electron-phonon coupling constant λ(q) as a function of the- Gaussian broadening σ for H_6SCl at **q** = (0, 0, 0) at c200 GPa. We believe that 12×12 ×12 *k*-meshes are converged in H_6SCl.

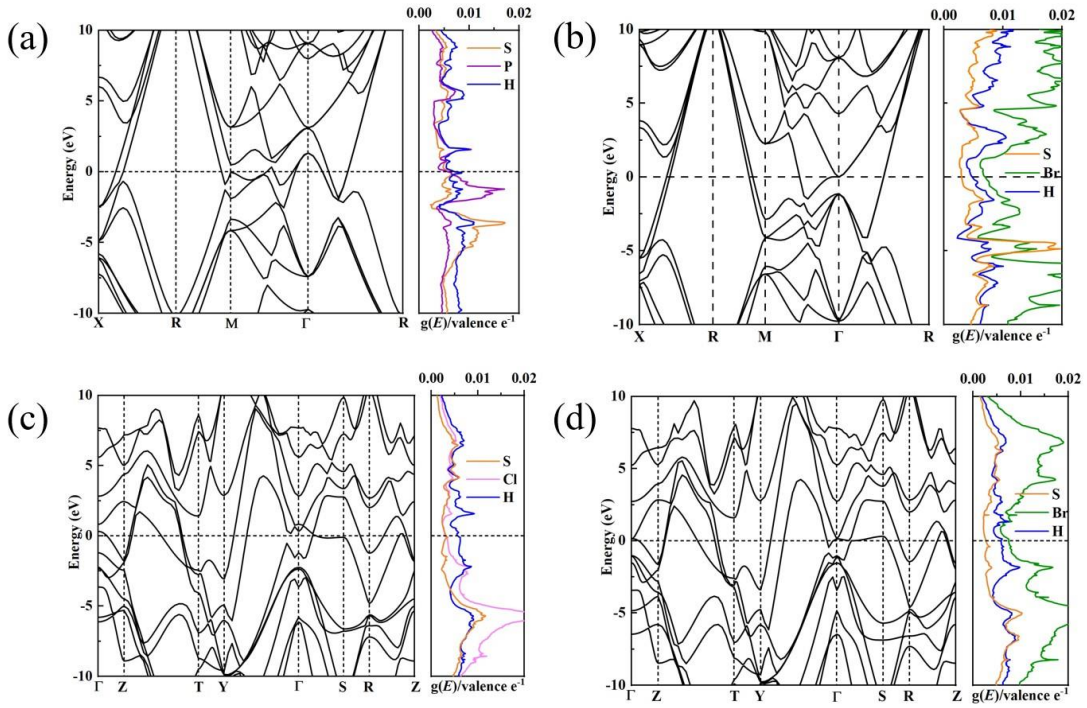

FIG. S2 Electronic band structure and DOS (states/eV/f.u.) of (a) $Pm\bar{3}m$-H_6SP at 200 GPa, (b) $Pm\bar{3}m$-H_6SBr at 200 GPa, (c) *Cmmm*-H_6SCl at 200 GPa and (d) *Cmmm*-H_6SBr at 200 GPa.

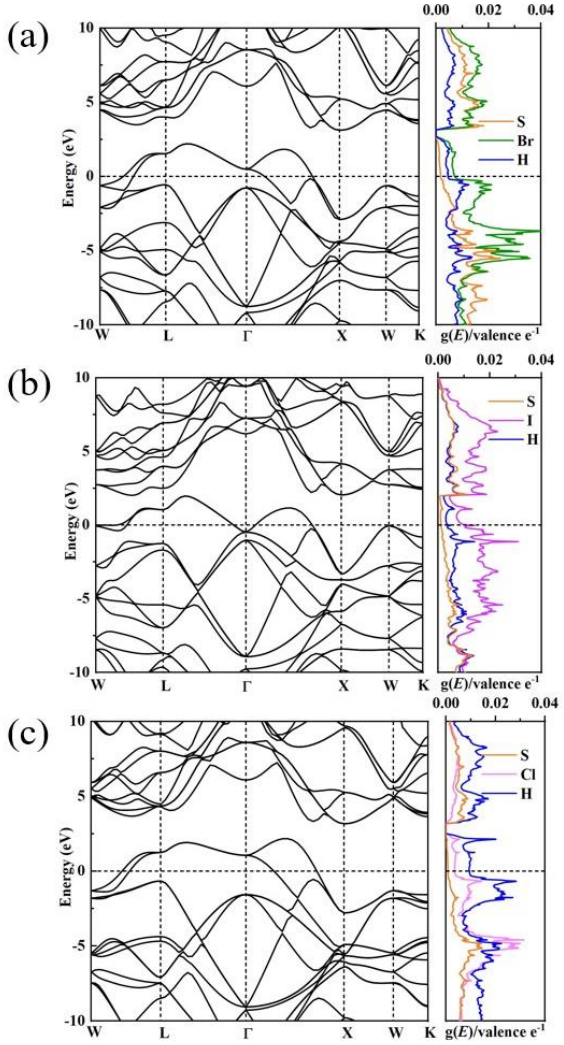

FIG. S3 Electronic band structure and DOS of (a) $Fd\bar{3}m$-H_6SBr at 200 GPa, (b) $Fd\bar{3}m$-H_6SI at 200 GPa, and (c) $Fd\bar{3}m$-H_6SCl at 200 GPa.

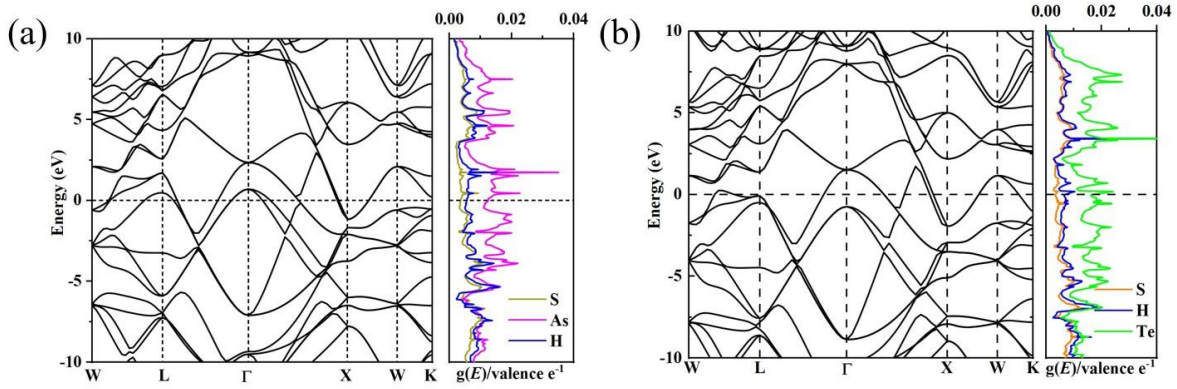

FIG. S4 Electronic band structure and DOS of (a) $Fd\bar{3}m$-H_6SAs at 200 GPa and (b) $Fd\bar{3}m$-H_6STe at 200 GPa.

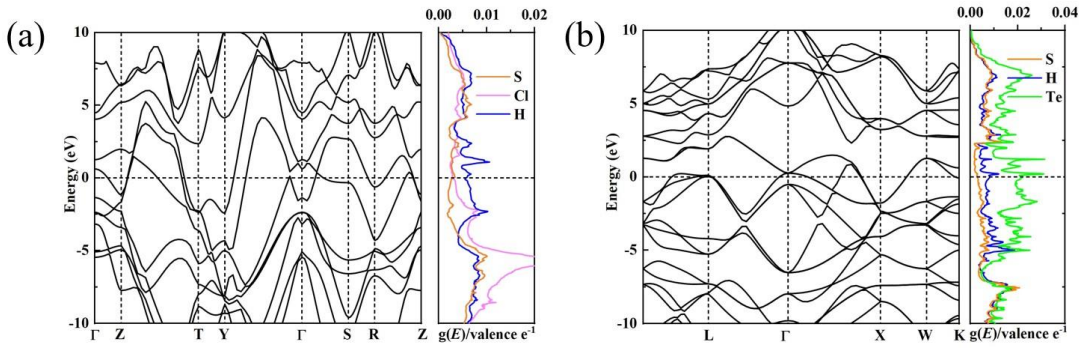

FIG. S5 Electronic band structure and DOS of (a) *Cmmm*-H_6SCl at 130 GPa and (c) $Fd\bar{3}m$-H_6STe at 100 GPa.

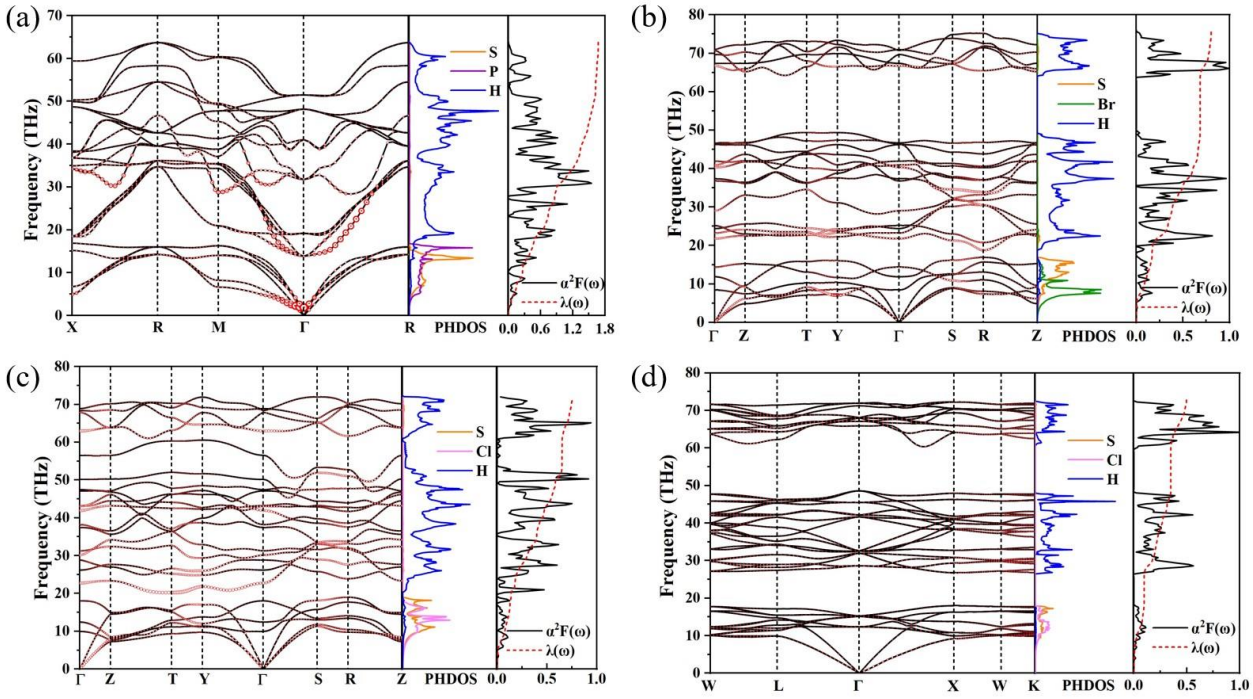

FIG. S6 Phonon spectra, phonon density of states, Eliashberg phonon spectral function $\alpha^2F(\omega)$, and the electron-phonon integral λ for (a) $Pm\bar{3}m$-H_6SP at 200 GPa, (b) *Cmmm*-H_6SBr at 200 GPa, (c) *Cmmm*-H_6SCl at 200 GPa and (d) $Fd\bar{3}m$-H_6SCl at 200 GPa.

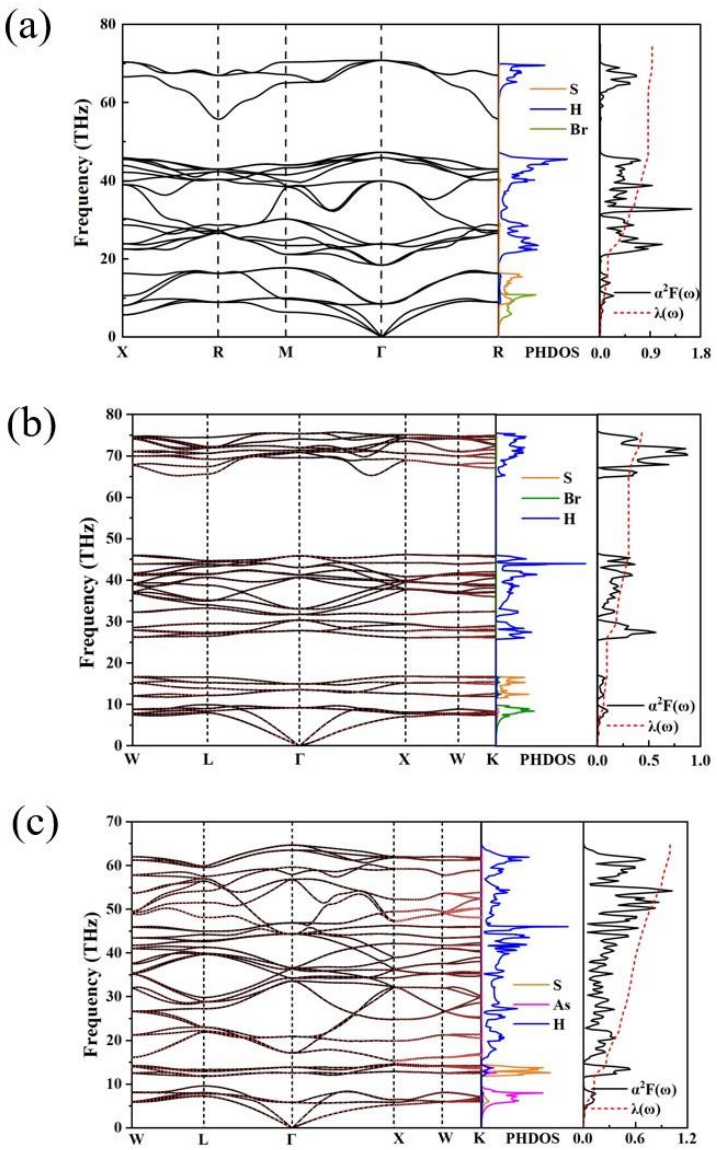

FIG. S7 Phonon spectra, phonon density of states, Eliashberg phonon spectral function $\alpha^2F(\omega)$, and the electron-phonon integral λ for (a) $Pm\bar{3}m$-H_6SBr at 200 GPa, (b) $Fd\bar{3}m$-H_6SBr at 200 GPa and (c) $Fd\bar{3}m$-H_6SAs at 200 GPa.

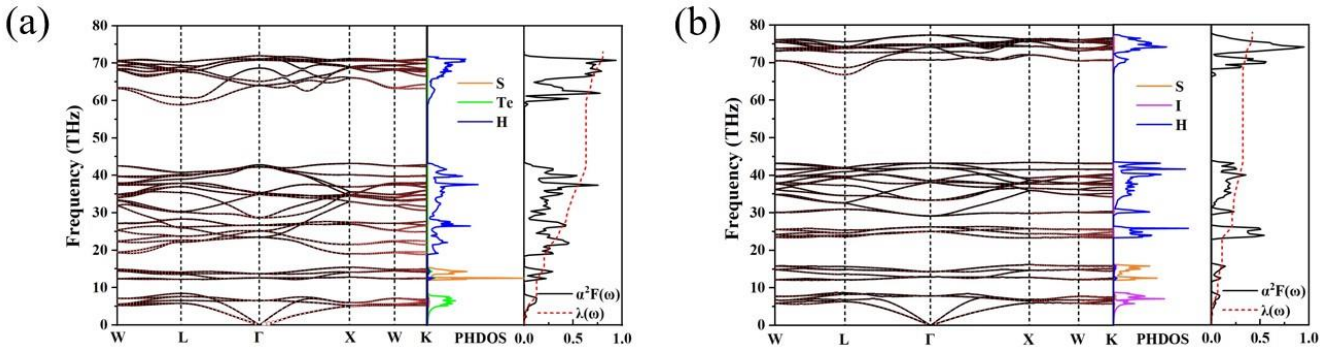

FIG. S8 Phonon spectra, phonon density of states, Eliashberg phonon spectral function $\alpha^2F(\omega)$, and the electron-phonon integral λ for (a) $Fd\bar{3}m$-H_6STe at 200 GPa and (b) $Fd\bar{3}m$-H_6SI at 200 GPa.

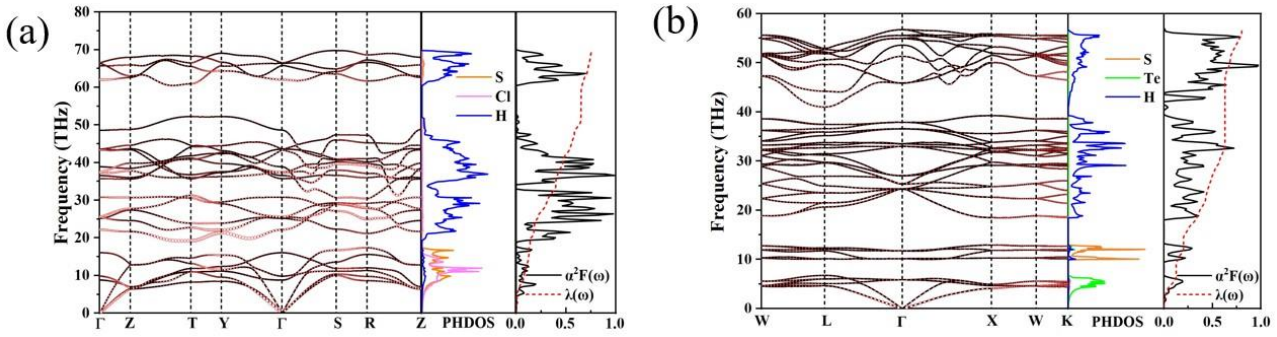

FIG. S9 Phonon spectra, phonon density of states, Eliashberg phonon spectral function $\alpha^2F(\omega)$, and the electron-phonon integral λ for (a) $Cmmm$-H_6SCl at 130 GPa and (b) $Fd\bar{3}m$-H_6STe at 100 GPa.

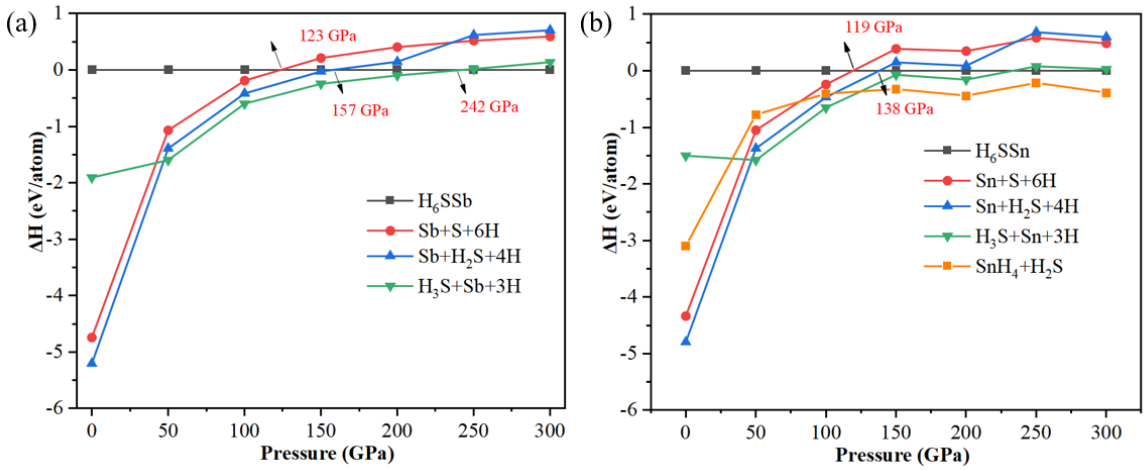

FIG. S10 Enthalpy difference vs pressure for (a) H_6SSb, referenced to the decomposition enthalpy into H_6SSb. The decomposition enthalpies into Sb + S + 6H, $Sb+H_2S+4H$ and $H_3S+Sb+3H$ were also plotted, respectively. (b) H_6SSn, referenced to the decomposition enthalpy into H_6SSn. The decomposition enthalpies into Sn + S + 6H, $Sn+H_2S+4H$, $H_3S+Sn+3H$ and SnH_4+H_2S were also plotted, respectively.

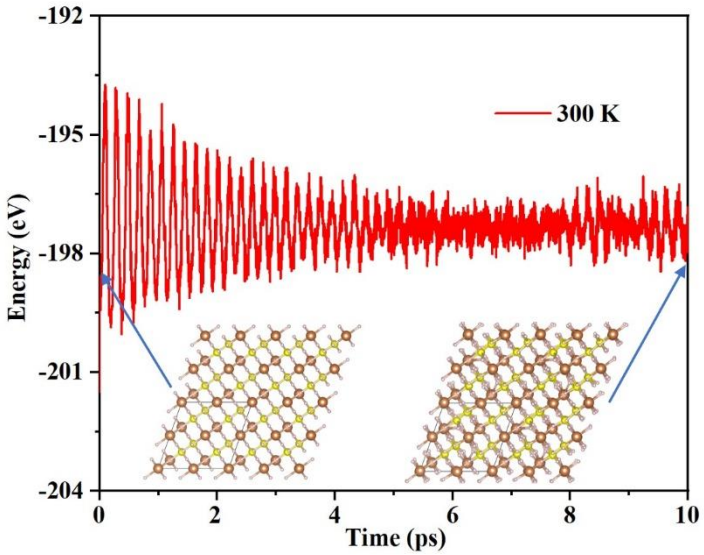

FIG. S11 the total free energy as a function of the ab initio molecular dynamics (AIMD) simulation time at 300 K under 200 GPa. The inset presents the structure snapshots of $Fd\bar{3}m$ H6SSb at 0 and 10 ps, respectively.

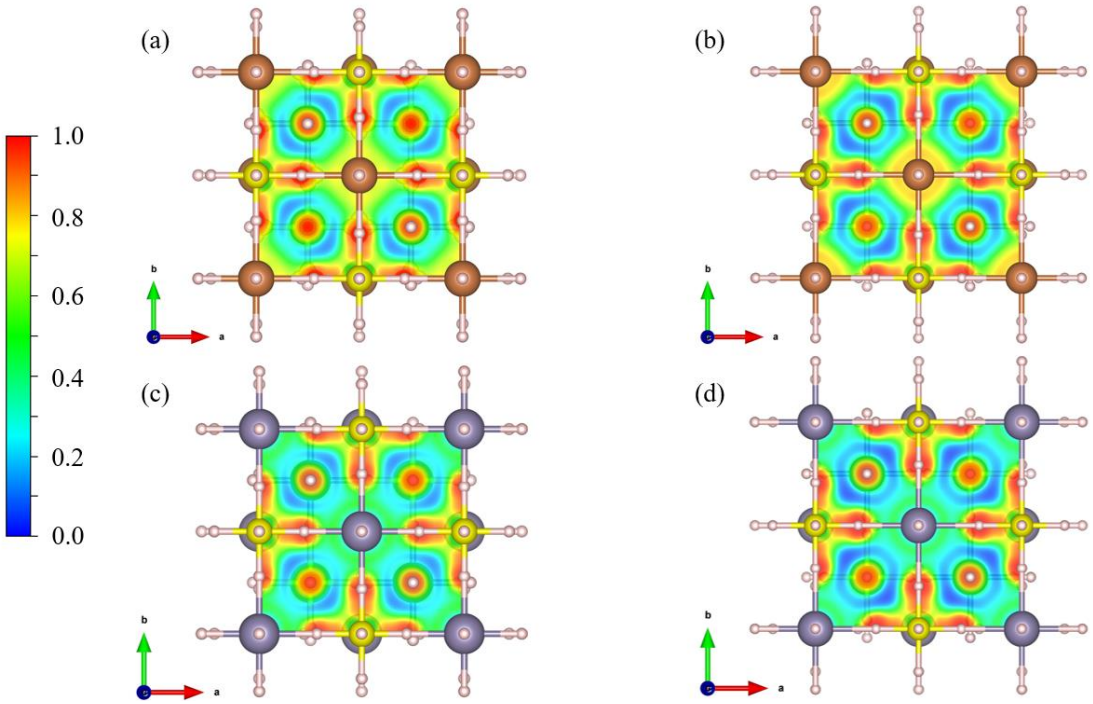

FIG. S12 Calculated electron localization function (ELF) of (a) $Fd\bar{3}m$-H_6SSb at 200 GPa, (b) $Fd\bar{3}m$-H_6SSb at 40 GPa, (c) $Fd\bar{3}m$-H_6SSn at 200 GPa and (d) $Fd\bar{3}m$-H_6SSn at 40 GPa.

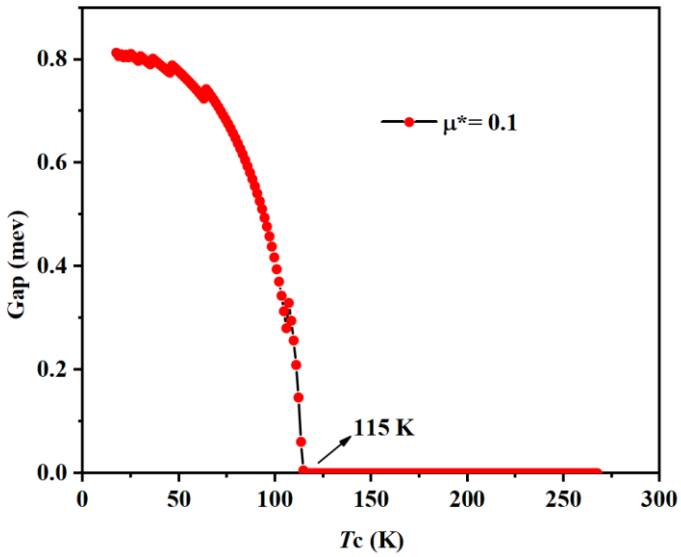

FIG. S13 Calculated anisotropic superconducting gap of H_6SSb in the $Fd\bar{3}m$ structure at 40 GPa.

Table. S1 The valence electrons of the atoms

	S	**H**	**Sn**	**P**	**As**	**Sb**	**Te**	**Cl**	**Br**	**I**
	s^2p^4	S^1	s^2p^2	s^2p^3	s^2p^3	s^2p^3	s^2p^4	s^2p^5	s^2p^5	s^2p^5